

## Effects of Diffusion on Free Precession in Nuclear Magnetic Resonance Experiments\*†

H. Y. CARR, *Department of Physics, Rutgers University, New Brunswick, New Jersey*

AND

E. M. PURCELL, *Lyman Laboratory of Physics, Harvard University, Cambridge, Massachusetts*

(Received January 19, 1954)

Nuclear resonance techniques involving free precession are examined, and, in particular, a convenient variation of Hahn's spin-echo method is described. This variation employs a combination of pulses of different intensity or duration ("90-degree" and "180-degree" pulses). Measurements of the transverse relaxation time  $T_2$  in fluids are often severely compromised by molecular diffusion. Hahn's analysis of the effect of diffusion is reformulated and extended, and a new scheme for measuring  $T_2$  is described which, as predicted by the extended theory, largely circumvents the diffusion effect. On the other hand, the free precession technique, applied in a different way, permits a direct measurement of the molecular self-diffusion constant in suitable fluids. A measurement of the self-diffusion constant of water at 25°C is described which yields  $D = 2.5(\pm 0.3) \times 10^{-5}$  cm<sup>2</sup>/sec, in good agreement with previous determinations. An analysis of the effect of convection on free precession is also given. A null method for measuring the longitudinal relaxation time  $T_1$ , based on the unequal-pulse technique, is described.

### I. INTRODUCTION

IN order to explain the spin-echo envelopes obtained from certain samples in his nuclear magnetic resonance free precession experiments, Hahn<sup>1</sup> found it necessary to consider the diffusion of the molecules through the inhomogeneous external field. Recent experiments using a somewhat modified free precession technique have allowed further observation and analysis of the diffusion effects. These studies are interesting for two reasons. First, they provide a firmer basis for the use of the free precession method in measuring nuclear magnetic relaxation times. Secondly, for suitable samples a relatively direct measurement of the diffusion coefficient is possible.

In order to introduce terminology and notation, the principles of the free precession method will be briefly reviewed. Hahn<sup>1</sup> has described typical apparatus. The only additional equipment used in our experiments consists of two independent pulse width controls and more flexible triggering circuits.

We will denote the total magnetic moment of the nuclear sample by the vector  $\mathbf{M}$ . At thermal equilibrium,  $\mathbf{M}$  is parallel to the strong applied field,  $\mathbf{H} = H_z \mathbf{k}$ , and its magnitude is given by the product of  $H_z$  and the static nuclear susceptibility. We denote this equilibrium value by  $M_0$ .

In describing the precessional motions of the nuclei of the sample it is necessary to take account of the inhomogeneity of the applied field. The fraction of the nuclei associated with a value of  $H_z$  in a small interval about a particular  $H_z$  will be denoted by  $f(H_z)dH_z$ .

The normalized distribution function  $f(H_z)$  is considered centered at  $H_z = H_{z0}$ . The field deviations are  $\Delta H_z = H_z - H_{z0}$ . The root-mean-square deviation  $\sigma$  may be used as a measure of the width of the distribution. With each value of  $H_z$  and with an increment  $dH_z$ , we associate an incremental magnetic moment  $d\mathbf{M}(H_z)$ , which is the vector sum of the moments of all nuclei within regions where the field strength is between  $H_z$  and  $H_z + dH_z$ . The motions of these incremental net magnetic moment vectors are described by the equation

$$\frac{d}{dt}d\mathbf{M}(H_z) = -\gamma \mathbf{H} \times d\mathbf{M}(H_z), \quad (1)$$

where  $\gamma$  the gyromagnetic ratio is the ratio of the magnetic moment to the nuclear angular momentum. Thus an incremental magnetic moment vector making a finite angle with  $\mathbf{H}$  will precess in a negative sense for  $\gamma > 0$  with angular frequency of magnitude  $\gamma|\mathbf{H}|$  about the direction of  $\mathbf{H}$ . In nuclear magnetic resonance studies it is customary to describe this precession in a rotating coordinate system in which all or part of the magnetic field is effectively eliminated. This procedure has been described elsewhere.<sup>2</sup> In the transformations used in our discussion only  $H_z$  or portions of  $H_z$  will be eliminated. For example, if  $d\mathbf{M}(H_{z0})$  makes an angle  $\theta$  with  $\mathbf{H} = H_{z0}\mathbf{k}$ , it will precess in the laboratory coordinate system about the  $z$  axis with angular frequency having magnitude  $\gamma H_{z0}$ . By transforming to a rotating coordinate system having the angular frequency  $\boldsymbol{\Omega} = -\gamma H_{z0}\mathbf{k}$ ,  $d\mathbf{M}(H_{z0})$  will appear stationary, as though  $H_{z0}$  had been eliminated. This may also be seen from the transformation equation

$$\frac{\delta}{\delta t}d\mathbf{M}(H_{z0}) = -\gamma \left( \mathbf{H} + \frac{\boldsymbol{\Omega}}{\gamma} \right) \times d\mathbf{M}(H_{z0}). \quad (2)$$

\* This work was partially supported by the joint program of the U. S. Office of Naval Research and the U. S. Atomic Energy Commission, by The Radio Corporation of America, by the Rutgers University Research Council, and by the United States Air Force under a contract monitored by the Office of Scientific Research, Air Research and Development Command.

† Portions of this work have been previously described by H. Y. Carr, thesis, Harvard University, 1952 (unpublished).

<sup>1</sup> E. L. Hahn, *Phys. Rev.* **80**, 580 (1950).

<sup>2</sup> R. K. Wangsness, *Am. J. Phys.* **21**, 274 (1953).

However, for the more general incremental vector  $dM(H_z)$  not all of the  $H_z$  is eliminated in the above rotating coordinate system. As a result,  $dM(H_z)$  precesses with the small angular frequency

$$\omega_{\Delta} = -\gamma(H_z - H_{z0})\mathbf{k}'.$$

This is illustrated in Fig. 1B.

In free precession experiments the radio-frequency energy is applied to the sample in short intense pulses. The rf magnetic field, as in other nuclear resonance methods, is applied to the sample at right angles to the strong static field. Its magnitude will be denoted by  $2H_1$ . The frequency of the rf field satisfies the resonant condition  $\omega_{rf} = \gamma H_{z0}$ . As is well known,<sup>3</sup> only one of the two circularly polarized components composing the linearly polarized rf field is effective in nutating the net magnetic moments. This component, with magnitude  $H_1$ , is the one which rotates in phase with the precessing moments. The phase of the rotating system will be so chosen that this  $H_1$  is along the  $x'$  axis. With the rf pulse applied, the net field  $\mathbf{H} = \Delta H_z \mathbf{k}' + H_1 \mathbf{i}'$  will determine the precession of the incremental moment vectors. This is illustrated in Fig. 1C. However, a special approximation is possible in the present work. The magnitude of the rf field is made so large ( $H_1 \gg \sigma$ ), and the duration of the rf pulse  $\tau_w$  so short ( $\tau_w \ll 1/\gamma\sigma$ ), that the precession about the net field is effectively equivalent to precession about  $H_1 \mathbf{i}'$ . This precession during the time the rf pulse is applied might be referred to as pure nutation. Furthermore, in the above approximation all incremental moments will rotate together as a single total magnetic moment vector. Figure 2A illustrates the combined precession about  $\mathbf{k}$  and nutation about  $\mathbf{i}$  as seen from the laboratory frame of reference while Fig. 2B illustrates the pure nutation about  $\mathbf{i}'$  as seen from the rotating frame of reference. In a time  $\tau_w$  the angle of nutation is  $\theta = \gamma H_1 \tau_w$ . In the present experiments only two angles of nutation are used. These are  $90^\circ$  and  $180^\circ$ . When the rf oscillator gating circuit is so adjusted that

$$\gamma H_1 \tau_w = \frac{1}{2}\pi, \quad (3)$$

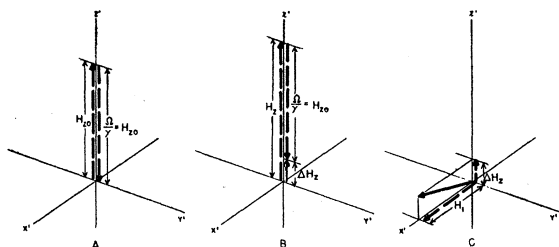


FIG. 1. The apparent elimination of  $H_z$  as viewed from a frame of reference rotating with the angular frequency  $\Omega = -\gamma H_{z0} \mathbf{k}$ . For  $H_z = H_{z0}$ , there is no resultant field (A); but in a general case (B), there is a resultant field  $\Delta H_z = H_z - H_{z0}$ . When the rf field  $H_1$  is applied,  $\Delta H_z$  combines with  $H_1$  to determine the direction (C) about which rotation occurs.

<sup>3</sup> G. E. Pake, Am. J. Phys. 18, 438 (1950).

the net magnetic moment vector will rotate through an angle  $\theta = \frac{1}{2}\pi$ , for example, from the polar  $z'$  axis down to the equatorial plane of the reference sphere. This is referred to as a  $90^\circ$  pulse. Similarly, if  $\tau_w$  is such that the vector rotates, for example, from the positive  $z'$  axis to the negative  $z'$  axis, one has a  $180^\circ$  pulse.

Consider a situation in which free precession is initiated with a  $90^\circ$  pulse. Following the removal of the pulse the total net magnetic moment precesses in the equatorial plane and induces a rf signal in the coil surrounding the sample. For liquid and gaseous samples this signal decays, in a time long compared to the  $\tau_w$  used in our experiments, because of the differences in the precessional frequencies of the incremental moment vectors. Viewed from the rotating frame of reference, the incremental moment vectors appear to fan out. This is illustrated in C and D of Fig. 3. The magnitude of the total magnetic moment vector, and hence the induced signal, is thereby reduced. The decaying nuclear signal following the  $90^\circ$  pulse is referred to as a "tail." For a symmetrical distribution function no  $x'$  component of the total moment vector exists. The  $y'$  component is given by

$$M_{y'} = M_0 \int f(H_z) \cos \gamma(H_z - H_{z0})t dH_z. \quad (4)$$

This expression describes the time dependence of the tail. For example, if the distribution is an error function, the tail has the form

$$M_{y'} = M_0 \exp(-\sigma^2 \gamma^2 t^2 / 2), \quad (5)$$

while if  $f(H_z)$  is a rectangular function of width  $2h$ ,

$$M_{y'} = M_0 [(\sin \gamma h t) / \gamma h t]. \quad (6)$$

Wide distributions correspond to fast decays and narrow, or more homogeneous distributions, to slow decays. This is illustrated in Fig. 4. If the distribution function consists of two or more distinct spin groups, such as those caused by different diamagnetic effects

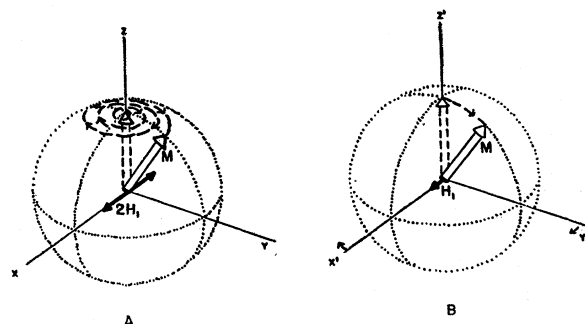


FIG. 2. (A) The combination of precession and nutation of the net magnetic moment as viewed from the laboratory frame of reference. (B) Pure nutation of the net magnetic moment as viewed from the frame of reference rotating at the precessional frequency.

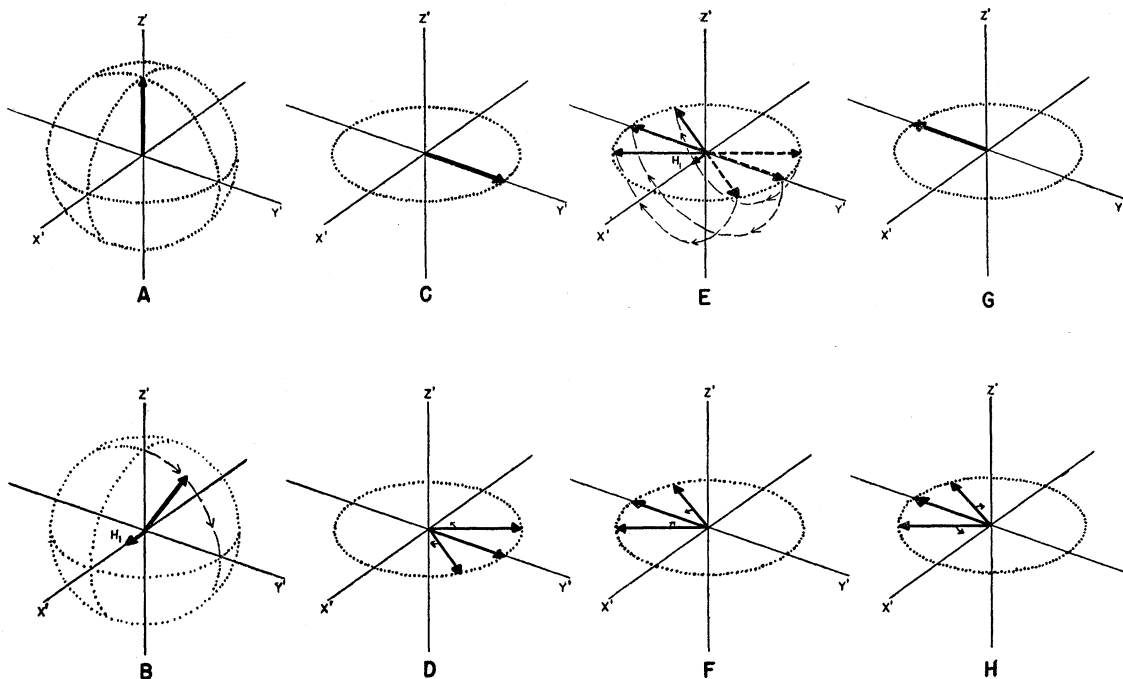


FIG. 3. The formation of an echo. Initially the net magnetic moment vector is in its equilibrium position (*A*) parallel to the direction of the strong external field. The rf field  $H_1$  is then applied. As viewed from the rotating frame of reference the net magnetic moment appears (*B*) to rotate quickly about  $H_1$ . At the end of a  $90^\circ$  pulse the net magnetic moment is in the equatorial plane (*C*). During the relatively long period of time following the removal of  $H_1$ , the incremental moment vectors begin to fan out slowly (*D*). This is caused by the variations in  $H_2$  over the sample. At time  $t = \tau$ , the rf field  $H_1$  is again applied. Again the moments (*E*) begin to rotate quickly about the direction of  $H_1$ . This time  $H_1$  is applied just long enough to satisfy the  $180^\circ$  pulse condition. This implies that at the end of the pulse all the incremental vectors are again in the equatorial plane. In the relatively long period of time following the removal of the rf field, the incremental vectors begin to recluster slowly (*F*). Because of the inverted relative positions following the  $180^\circ$  pulse and because each incremental vector continues to precess with its former frequency, the incremental vectors will be perfectly reclustered (*G*) at  $t = 2\tau$ . Thus maximum signal is induced in the pickup coil at  $t = 2\tau$ . This maximum signal, or echo, then begins to decay as the incremental vectors again fan out (*H*).

in different parts of a molecule, the tail will be modulated by their beat pattern. The tail in Fig. 5 illustrates such a beat pattern observed with a proton sample of acetic acid  $\text{CH}_3\text{COOH}$ .

## II. METHODS FOR MEASURING TRANSVERSE RELAXATION TIME

In liquids and gases the natural lifetimes of the nuclear signals ordinarily cannot be inferred from the decay of the tail. This decay is usually determined, as described above, by the inhomogeneous external field. However, by means of the spin-echo effect discovered by Hahn, this artificial decay can be effectively eliminated and the natural decay of the nuclear signal observed. The spin-echo effect is associated with the successive application of two or more rf pulses. Hahn has described the effect for equal pulse widths. In the present work combinations of  $90^\circ$  and  $180^\circ$  pulses have been used. This greatly simplifies the explanation of the effect and the interpretation of the observed data.

To obtain an echo using this technique, a  $180^\circ$  pulse is applied at a time  $\tau$  after the  $90^\circ$  pulse.  $\tau$  is chosen

larger than the artificial decay time of the tail but smaller than the natural lifetime of the nuclear signal. As illustrated in *E* of Fig. 3, the incremental vectors rotate  $180^\circ$  about the  $x'$  axis. When the rf field is removed at the end of the pulse, all incremental vectors are again in the equatorial plane. Since it is assumed that each nucleus remains in the same  $H_2$ , each will continue to precess in the same sense and with exactly the same angular frequency as it did before the  $180^\circ$  pulse. Because of this memory and because of their new relative positions after the  $180^\circ$  pulse, the incremental moment vectors will all recluster together in exactly  $\tau$  units of time after the  $180^\circ$  pulse. This is at time  $2\tau$ . At this time there will be a maximum total magnetic moment vector and hence maximum induced signal or an echo. Following  $t = 2\tau$  the incremental vectors again fan out, and the echo decays in the same manner that it formed. An echo simply appears as two tails back to back. This is vividly illustrated by the echo in Fig. 5.

In order to utilize the above effect in observing the natural lifetimes of nuclear signals, Hahn introduced a method of measurement which will be referred to as

Method *A*. In this method the amplitude of the echo following a single two-pulse sequence is plotted as a function of time. The data for the different points are obtained by using different values of  $\tau$ .

The plot may be made photographically by taking a multiple exposure picture of the oscilloscope screen displaying the detected nuclear signals. Each exposure corresponds to a different two-pulse sequence and echo at  $2\tau$ . The envelope of the photographed echoes is the desired curve. From considerations mentioned thus far, one would expect that this plot would indicate the natural decay or lifetime of the transverse polarization  $M_{y'}$ .

This natural decay is expected to proceed exponentially. It is caused, if one restricts the discussion to nuclei without electric quadrupole moments, by the local magnetic field which originates in moments carried by neighboring atoms and molecules. Owing to the Brownian motion of these other dipoles as well as that of the nucleus in question, this local magnetic field varies randomly both in magnitude and in direction.<sup>4</sup> In liquids and gases the variation is usually so much more rapid than the Larmor precession that the local field has practically the same character whether viewed from the stationary or the rotating frame of reference. In this case it is easy to understand what happens. A moment directed originally along the  $y'$  axis, exposed to this random field, executes on the reference sphere a random walk made up of very short steps. The whole cluster of moments thus spreads by diffusion over the

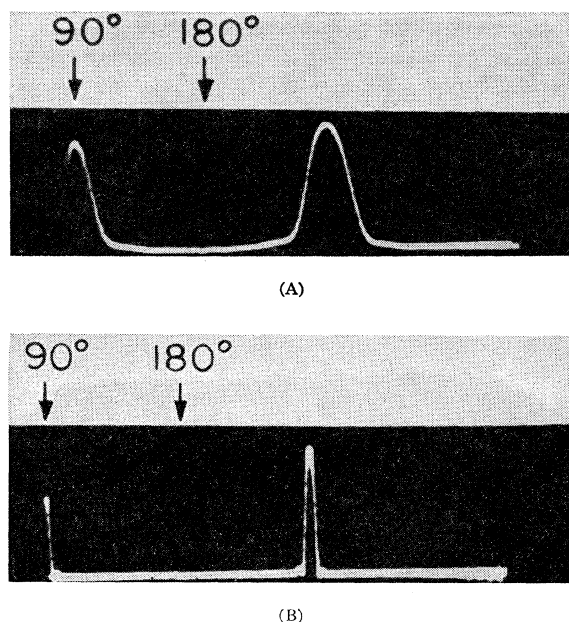


FIG. 4. Effect of the homogeneity of the field on the widths of tails and echoes. The tails and echoes associated with a sample (A) in a very homogeneous field are wide compared to those associated with a sample (B) in a less homogeneous field.

<sup>4</sup> Bloembergen, Purcell, and Pound, Phys. Rev. **73**, 679 (1948).

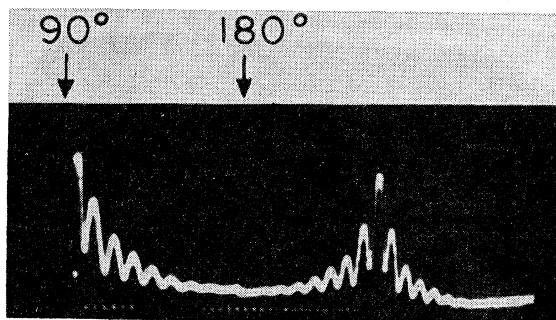


FIG. 5. A tail and echo associated with an acetic acid ( $\text{CH}_3\text{COOH}$ ) sample in a very homogeneous field. The nuclear signal displays modulation typical of the beating of two signals of nearly equal frequencies, the magnitude of one being three times that of the other. The beat frequency shown, corresponding to room temperature and 7000 gauss, is approximately 220 cps.

sphere. The exponential decay follows as a direct and general result. To illustrate with a simple if somewhat artificial model, suppose that the local field  $\mathbf{h}$  at a given nucleus changes exactly once every  $\tau_c$  seconds to a new magnitude and direction randomly selected. The other nuclei experience similar, but uncorrelated, variations in their local fields. It is then easy to show that

$$M_{y'}(t) = M_0 \exp(-\gamma^2 \langle h^2 \rangle_{Av} \tau_c t / 3), \quad (7)$$

where

$$\langle h^2 \rangle_{Av} = \langle h_x^2 \rangle_{Av} + \langle h_y^2 \rangle_{Av} + \langle h_z^2 \rangle_{Av}. \quad (8)$$

Many other approaches lead to the same result.<sup>5,6</sup>

In the cases of certain samples the echo envelopes obtained by Hahn's method, Method *A*, have essentially the above exponential form. However, for certain other nonviscous samples such as pure water the envelope is more nearly of the form  $\exp(-kt^2)$ . See Fig. 7A. Hahn was successful in showing that this is the form of the decay to be expected if the decay is caused by diffusion of the molecules through the inhomogeneous external field  $H_z$ . Therefore if diffusion is important, a decay or relaxation time measured by Method *A* is "artificially" determined by the external magnet.

In the present work a new method for obtaining an echo envelope which reveals the "natural" decay even in the presence of diffusion has been introduced. This method of measurement will be referred to as Method *B*. In Method *A* a number of  $90^\circ$  pulses must be applied to the sample in order to obtain sufficient data to plot the envelope. Each  $90^\circ$  pulse is followed by an  $180^\circ$  pulse and the accompanying echo. Between each  $90^\circ$ - $180^\circ$  sequence sufficient time must elapse to allow the sample to return to its thermal equilibrium condition. In Method *B* a single  $90^\circ$  pulse is used to obtain an entire echo envelope without requiring the sample to return to thermal equilibrium. This is accomplished by initiating the measurement with the usual  $90^\circ$  pulse at  $t=0$ . A  $180^\circ$  pulse is then applied at time  $t=\tau$ . The

<sup>5</sup> R. K. Wangsness and F. Bloch, Phys. Rev. **89**, 728 (1953).

<sup>6</sup> A. Abragam and R. V. Pound, Phys. Rev. **92**, 943 (1953).

usual echo appears at time  $t=2\tau$ . Next, to illustrate with a particularly simple case, an additional  $180^\circ$  pulse is applied at time  $t=3\tau$ . By reasoning identical to that previously used in connection with the first echo, it can be seen that the incremental vectors will recluster at time  $t=4\tau$ . Thus, a second echo is formed. If this process is continued throughout the natural lifetime of the nuclear signal, additional echoes of decreasing amplitude are formed. The envelope of these echoes

indicates the decay of the polarization in the equatorial plane. In some experiments as many as 30 echoes have been formed following a single  $90^\circ$  pulse. Methods *A* and *B* are compared in Fig. 6.

In the case of viscous samples with negligible diffusion, the echo envelope obtained by Method *A* is identical to that obtained by Method *B*. This is not so if certain nonviscous samples are used. Figure 7 vividly illustrates the difference in envelopes obtained by the two methods if a water sample is used. The top photograph illustrating Method *A* is a multiple exposure picture of a series of thirteen  $90^\circ$ - $180^\circ$  pulse sequences, each with an accompanying echo at a different time  $2\tau$ . The decay is of the form  $\exp(-kt^2)$ . The time constant is approximately 0.2 sec. The lower photograph is a single exposure picture of a single sequence of pulses consisting of one  $90^\circ$  pulse followed by fifteen  $180^\circ$  pulses. The decay is of the form  $\exp(-Kt)$ . The time constant is approximately 2.0 sec!

### III. THE EFFECT OF DIFFUSION

The above difference between Method *A* and Method *B* may be explained by analyzing the effect of the molecular diffusion on the distribution-in-phase of the precessing moments. One may replace the diffusion by a random walk of discrete steps. This makes it easier to formulate certain parts of the problem. As we shall pass finally to the limit of infinitesimal steps, introducing at that point the ordinary molecular self-diffusion constant  $D$ , the details of the random walk model are not critical. For simplicity we assume a random walk of the following sort: a molecule remains at a given  $z$  position for exactly  $\tau$  seconds, when it abruptly jumps to a new position whose  $z$  coordinate differs from the previous one by  $\zeta a_i$ , where  $\zeta$  is a fixed distance and  $a_i$  a random variable whose value is 1 or  $-1$ . The constant linear gradient is in the  $z$  direction.  $\zeta$  might more properly be defined by  $(\langle z_i^2 \rangle_{Av})^{1/2}$ , the rms  $z$  component of a three-dimensional jump of magnitude  $\delta = (3\langle z_i^2 \rangle_{Av})^{1/2}$ .

The effect we are interested in is the change in the rate of nuclear precession, and the resulting discrepancy in phase, caused by the transport of the nucleus into a region where the applied field is slightly different. Let the gradient of  $H_z$  in the  $z$  direction be constant, and, in magnitude,  $G$  gauss/cm, and let  $H_z(0)$  be the field in which a given nucleus finds itself at  $t=0$ . At some later time  $t=j\tau$  the nucleus will find itself in a field  $H_z(j\tau)$  given by

$$H_z(j\tau) = H_z(0) + G\zeta \sum_{i=1}^j a_i.$$

After  $N$  steps, that is after a time  $t=N\tau$ , the phase  $\phi$  of the precessing moment of this nucleus will differ from the value  $\phi_0$  it would have had at this same instant if the nucleus had remained in the same place by an

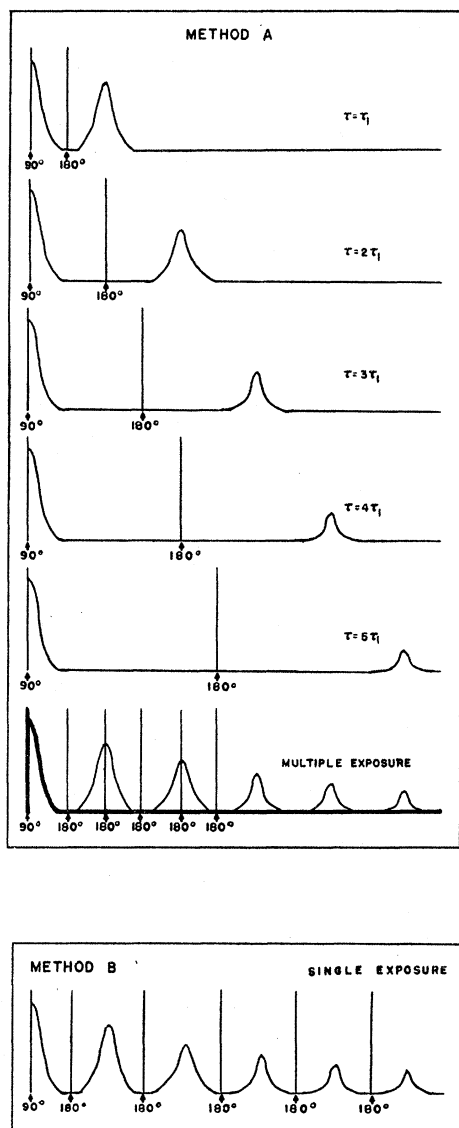


FIG. 6. Comparison of the two free precession methods for observing the decay time of the horizontal component of nuclear magnetic polarization. In "Method *A*" the sample must return to its equilibrium condition each time an additional echo is to be observed. In "Method *B*" the sample need only start from equilibrium once. The separate oscilloscope traces of "Method *A*" are usually displayed superimposed in a multiple exposure picture. Only a single trace and hence a single exposure picture is required in "Method *B*." However this latter method requires more than one  $180^\circ$  pulse.

angle

$$\begin{aligned}\phi_D &= \phi - \phi_0 = \sum_{j=1}^N \gamma\tau [H_z(j\tau) - H_z(0)] \\ &= G\zeta\gamma\tau \sum_{j=1}^N \sum_{i=1}^j a_i = G\zeta\gamma\tau \sum_{j=1}^N (N+1-j)a_j. \quad (10)\end{aligned}$$

As the  $a_j$ 's are random variables anyway, the last sum can just as well be written

$$G\zeta\gamma\tau \sum_{j=1}^N ja_j. \quad (11)$$

Now it can be shown that the central limit theorem holds for this sum. Therefore, if at time  $t=N\tau$  we consider the distribution in phase of an ensemble of moments, we can assert that the distribution will be Gaussian in the limit of large  $N$ . It only remains to calculate  $\langle \phi_D^2 \rangle_{Av}$ . This is easily done:

$$\begin{aligned}\langle \phi_D^2 \rangle_{Av} &= G^2\zeta^2\gamma^2\tau^2 \sum_{j=1}^N j^2 \\ &= G^2\zeta^2\gamma^2\tau^2 N(N+1)(2N+1)/6. \quad (12)\end{aligned}$$

If  $N$  is large—and in this problem it is in fact enormous—we may not only drop the lower powers of  $N$ , but we may at the same time pass over to a description in terms of a continuous diffusion rather than discrete random steps. By comparing the solution to the diffusion equation  $D\nabla^2 f = \partial f / \partial t$ , where  $f(x, y, z)$  is the probability density, with the solution to the random walk problem of the assumed type, it is easy to show that the appropriate diffusion constant is

$$D = \delta^2 / 6\tau = \zeta^2 / 2\tau. \quad (13)$$

We thus have

$$\langle \phi_D^2 \rangle_{Av} = 2G^2\gamma^2 D t^3 / 3, \quad (14)$$

and for the distribution-in-phase after time  $t$  we have

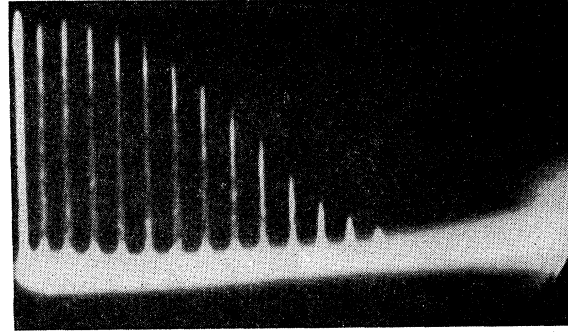
$$P(\phi_D) = (4\pi\gamma^2 G^2 D t^3 / 3)^{-1/2} \exp(-3\phi_D^2 / 4G^2\gamma^2 D t^3). \quad (15)$$

This is identical with the result given by Hahn,<sup>1</sup> and it applies directly to the behavior of the signal in the tail after a  $90^\circ$  pulse.

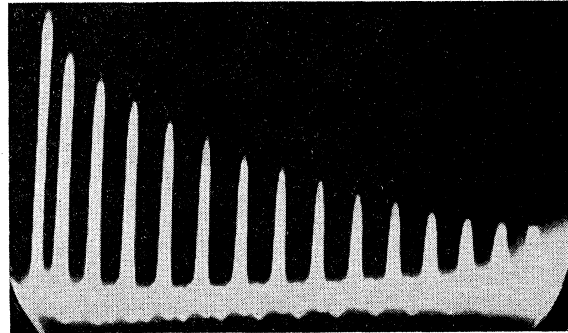
We now extend the analysis to the case in which a number of  $180^\circ$  pulses are applied after the initial  $90^\circ$  pulse. Let the  $90^\circ$  pulse occur at  $t=0$  as before. If we return to the discrete model, the effect of a  $180^\circ$  pulse applied at  $t=t_1$ , for example, is simply to *reverse the signs* of all terms in

$$\phi_D = \sum_{j=1}^N \gamma\tau [H_z(j\tau) - H_z(0)] \quad (16)$$

beyond  $j=t_1/\tau$ . Let us specialize at once to the interesting case in which, within the whole interval  $t=N\tau$ ,  $n$   $180^\circ$  pulses are applied; the first at  $t=N\tau/2n$ , the second at  $t=3N\tau/2n$ , and so on. Echoes will then occur midway between the  $180^\circ$  pulses and, in particular, an



(A)



(B)

FIG. 7. (A) A "Method A" decay associated with water at  $25^\circ\text{C}$ . The time constant is approximately 0.2 sec. The decay is largely determined by the molecular diffusion through the 0.28 gauss/cm gradient. The decay is dominated by the factor  $\exp(-kt^3)$ . (B) A "Method B" decay associated with water at  $25^\circ\text{C}$ . The time constant of the decay is approximately 2.0 sec. The effect of diffusion has been largely circumvented.

echo will occur at  $t=N\tau$ . We are interested in finding the effect of diffusion on this final echo. For this case we must now rewrite  $\phi_D$  as

$$\phi_D = \phi - \phi_0 = G\zeta\gamma\tau \sum_{j=1}^N b_j \sum_{i=1}^j a_i, \quad (17)$$

where

$$\begin{aligned}b_j &= 1 \quad \text{for } 0 < j \leq N/2n, \quad 3N/2n < j \leq 5N/2n, \text{ etc.}, \\ b_j &= -1 \quad \text{for } N/2n < j \leq 3N/2n, \quad 5N/2n < j \leq 7N/2n, \text{ etc.}\end{aligned}$$

By writing out the terms in an array, it is easy to see that the above double sum involving the random variables can be replaced by the sum of  $n$  independent sums of the type  $\sum_{k=1}^{(N/2n)-1} ka_k$ , and  $n$  independent sums of the type  $\sum_{k=1}^{N/2n} ka_k$ . We thus find at once that

$$\langle \phi_D^2 \rangle_{Av} = G^2\zeta^2\gamma^2\tau^2 [(N^3/12n^2) - N/6], \quad (18)$$

or, in the limit of large  $N$ , by

$$\langle \phi_D^2 \rangle_{Av} = G^2\gamma^2 D t^3 / 6n^2, \quad (n \neq 0). \quad (19)$$

The effect of interpolating a larger number  $n$  of  $180^\circ$  pulses in the interval of duration  $t$  is to reduce the mean square phase dispersion by a factor determined

by  $1/n^2$ . As far as diffusion is concerned, the intensity of the echo at time  $t$  is determined by

$$M_{y'}(t) = M_0 \int_{-\infty}^{+\infty} \cos \phi_D P(\phi_D) d\phi_D \\ = M_0 \exp(-\gamma^2 G^2 D t^3 / 12 n^2). \quad (20)$$

Thus decay caused by diffusion can theoretically be eliminated by simply making  $n$  large enough. If the effect of the natural decay is included we have

$$M_{y'}(t) = M_0 \exp[-(t/T_2) + (-\gamma^2 G^2 D t^3 / 12 n^2)]. \quad (21)$$

This quantitative theory successfully explains the echo amplitudes obtained in both Method *A* and Method *B*. The form of the envelope obtained in Method *A* is given when  $n=1$ . There is a difference in numerical factors in the exponent of the above result and the result given by Hahn.<sup>1</sup> Hahn did not take into account the effectiveness of the  $180^\circ$  pulse in partially eliminating the artificial decay caused by the diffusion.

#### IV. MEASUREMENT OF A DIFFUSION CONSTANT

As an application of the above considerations, the diffusion coefficient of water at  $25^\circ\text{C}$  has been measured. To do this Method *A* was used to observe the decay of the transverse polarization. Water is a suitable sample for such an experiment. This is determined from the values of  $T_2$  and  $D$ . For the effect to be pronounced one must require that

$$12/\gamma^2 G^2 D \leq T_2^3. \quad (22)$$

A gradient  $G$  may be obtained at the sample by placing symmetrically on either side of the sample two long current carrying wires or two circular turns of wire. The current directions should be such that the fields oppose. It is not sufficient to satisfy the above condition by simply increasing  $G$ . One must keep  $G$  small enough to insure that the condition  $H_1 \gg \sigma$  of Sec. I is also satisfied. This implies that our analysis in terms of simple  $90^\circ$  and  $180^\circ$  pulses is applicable. Furthermore, if one uses the value of  $G$  calculated from the current in the wires, it is necessary that this  $G$  be large compared to the average gradient of the field due to the magnet. To satisfy this condition, it is wise to search for a very homogeneous spot in the magnet.

In our measurements  $H_1$  was the order of 10 gauss. This can be determined by measuring  $\tau_w$  for a  $90^\circ$  pulse. The average gradient of the field due to the magnet was approximately 0.03 gauss/cm. This value can be determined either from the width of a tail following a  $90^\circ$  pulse, or from a Method *A* envelope with no current flowing in the parallel wires or the circular turns. Since a typical sample dimension is  $\frac{1}{2}$  cm, it can be seen that a gradient the order of  $\frac{1}{2}$  gauss/cm would satisfy both of the above conditions relating directly to  $G$ .  $T_2$  for water at  $25^\circ\text{C}$  has been measured by Method *B*. Diffusion effects were thus eliminated.  $T_2$  has a

value of 2.4 sec.  $D$  for water at this temperature is the order of  $2 \times 10^{-5}$  cm<sup>2</sup>/sec. With this information available it can be seen that condition (22) is also satisfied.

The value of the diffusion constant for water at  $25^\circ\text{C}$  as determined by this nuclear resonance method is  $2.5(\pm 0.3) \times 10^{-5}$  cm<sup>2</sup>/sec. The error which is indicated is the estimated maximum limit of error. This result is in good agreement with previous determinations.<sup>7</sup> The slope of a plot of  $\ln(M_{y'}/M_0) + t/T_2$  vs  $t^3$  is used to obtain  $D$ . Errors in determining this slope introduce the major portion of the uncertainty in the final value of  $D$ . For increasing values of the gradient, the experimental curve follows the straight line given by the assumed theory less well. Errors associated with the determination of the slope become greater. A gradient of 0.28 gauss/cm was used in the above determination.

The second important source of error occurs in the determination of the gradient. The gradient may be calculated from the current in the wires and the geometrical dimensions of the circuits. Corrections for the image currents in the pole faces of the magnet must be included. The estimated error in the calculation of the gradient is 2 percent. If one uses two circular turns or rings of current creating opposing fields, the gradient may be made very uniform over the volume of the sample by making the square of the diameter of the rings equal to  $4/3$  times the square of the ring separation. Such a uniform gradient may be measured quite directly by a second method. This involves the observation of the modulation of a tail following a  $90^\circ$  pulse. For a rectangular sample the tail has a form given by Eq. (6) of Sec. I. For a cylindrical sample the tail has the form

$$M_{y'} = M_0 2 J_1(\frac{1}{2} \gamma G d t) / \frac{1}{2} \gamma G d t, \quad (23)$$

where  $J_1(\frac{1}{2} \gamma G d t)$  is the first-order Bessel function and  $d$  is the diameter of the sample. The value of  $G$  obtained by this method has an estimated maximum limit of error of 5 percent. The values obtained by the two methods agree within experimental error.

It should be noted that this method for measuring the diffusion constant is apt to fail if the echo envelope exhibits modulation.<sup>8</sup> Such modulation is likely to occur if the resonant nucleus interacts with another nucleus of the same species which is in a chemically non-equivalent position in the molecule. It also sometimes occurs when the resonant nucleus interacts with another nucleus of a different species.

All methods for measurement of diffusion depend on somehow "labelling" molecules. To the extent that the "label" has a negligible effect on the diffusion process itself, a method may be said to measure truly the "self-diffusion" constant. In the method here described a molecule is in effect labelled by the direction of the nuclear magnetic moment it carries; a more innocuous label would be difficult to imagine.

<sup>7</sup> W. J. C. Orr and J. A. V. Butler, *J. Chem. Soc.* **1935**, 1273.

<sup>8</sup> E. L. Hahn and D. E. Maxwell, *Phys. Rev.* **88**, 1070 (1952).

## V. THE EFFECT OF CONVECTION

With any method for measuring the diffusion coefficient, it is desirable to be able to check that convection effects are not present. Fortunately we have such a check readily available here. If convection currents exist, the second echo of Method *B* may be larger than the first echo! This effect is most conspicuous when  $\tau_2$ , the time between the first and second  $180^\circ$  pulses, is exactly equal to  $2\tau_1$ , where  $\tau_1$  is the time between the  $90^\circ$  pulse and the first  $180^\circ$  pulse. This is illustrated in Fig. 8.

A mathematical explanation of the effect is easily given. Consider the changing phase angle of a group of nuclei which are moving uniformly into larger values of the external field of  $H_z$ . For the short distances which the nuclei move in the time between rf pulses, one may assume that the field gradient is linear. Assume that the field increases by  $h$  units per unit time. At time  $\tau_1$  the net magnetic moment vector of these nuclei will have in the rotating coordinate system a phase angle given by

$$\phi = \int_0^{\tau_1} \gamma(\Delta H_z + ht) dt = \gamma \Delta H_z \tau_1 + \frac{1}{2} \gamma h \tau_1^2 = \phi_0 + \phi_C. \quad (24)$$

$\phi_0$  is the phase angle which the moment vector would have had if it had remained stationary. However, the vector is out of phase by  $\frac{1}{2} \gamma h \tau_1^2$  radians more than  $\phi_0$ . Since this portion of the phase angle is due to convection, it will be denoted by  $\phi_C$ . After a  $180^\circ$  pulse is applied at  $t = \tau_1$ , the phase angle begins to decrease in magnitude. At time  $t = 2\tau_1$  the stationary component has been exactly compensated for, and  $\phi_0$  vanishes. However  $\phi_C$ , being proportional to  $t^2$ , has more than compensated for the value it obtained between 0 and  $\tau_1$ . It now has the value

$$\phi_C = \int_{\tau_1}^{2\tau_1} \gamma h t dt - \frac{1}{2} \gamma h \tau_1^2 = \gamma h \tau_1^2. \quad (25)$$

As time continues, both  $|\phi_0|$  and  $|\phi_C|$  increase. At time  $\tau_1 + \tau_2$  just before the second  $180^\circ$  pulse is applied, the value of  $\phi_C$  is given by

$$\phi_C = \int_{\tau_1}^{\tau_1 + \tau_2} \gamma h t dt - \frac{1}{2} \gamma h \tau_1^2 = \frac{1}{2} \gamma h (\tau_1 + \tau_2)^2 - \gamma h \tau_1^2. \quad (26)$$

In addition to this, the moment is out of phase by the stationary amount  $\phi_0$ . The second  $180^\circ$  pulse is then applied, and again the phase angles begin to decrease in magnitude. At the time  $t = 2\tau_2$ ,  $\phi_0$  will have been reduced to zero, but the convection will have caused  $\phi_C$  to change by an amount

$$\int_{\tau_1 + \tau_2}^{2\tau_2} \gamma h t dt = 2\gamma h \tau_2^2 - \frac{1}{2} \gamma h (\tau_1 + \tau_2)^2 \quad (27)$$

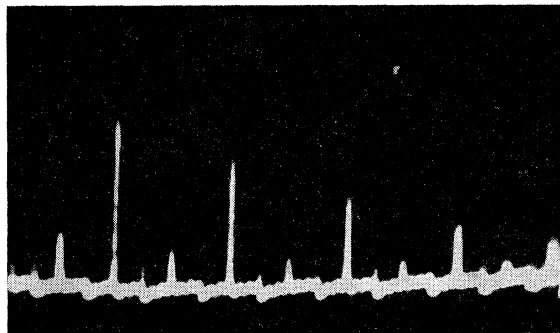


FIG. 8. The effect of molecular convection on a "Method *B*" decay. The odd-numbered echoes are much smaller than the even-numbered echoes.

radians. Thus, at time  $t = 2\tau_2$ , when the second echo normally occurs, the phase of the net magnetic moment will be given by  $\varphi = \varphi_0 + \varphi_C$ , where

$$\varphi_0 = 0, \quad \varphi_C = \gamma h \tau_2^2 - 2\gamma h \tau_1 \tau_2. \quad (28)$$

It is clear that it is possible to have all moments perfectly reclustered or in phase, at the time of the second echo, if  $\tau_2 = 2\tau_1$ . Such perfect reclustered is not possible at the time of the first echo because of the variations in  $h$  over the sample. This implies that with  $\tau_2 = 2\tau_1$ , the second echo may have a larger amplitude than the first, in agreement with the observed effect. Thus this effect can be used as an indicator of the presence of convection.

## VI. A METHOD FOR MEASURING THE LONGITUDINAL RELAXATION TIME

All discussion thus far has dealt with the equatorial or horizontal component of polarization and the associated relaxation time  $T_2$ . In conclusion, it will be mentioned that the use of  $90^\circ$  and  $180^\circ$  pulses makes possible a null method for the measurement of the longitudinal or spin-lattice relaxation time of the sample. This type of measurement is initiated by a  $180^\circ$  pulse. The total magnetic moment vector is inverted from the north pole to the south pole of the reference sphere. Because of the spin-lattice relaxation processes, the  $z$  component begins to return to its original value. A  $90^\circ$  pulse is then applied at various times  $\tau$ . For very short values of  $\tau$  the  $90^\circ$  pulse nutates the total magnetic moment vector of nearly maximum amplitude from the south pole to the equatorial plane. A tail with nearly maximum amplitude follows the  $90^\circ$  pulse. For very large values of  $\tau$ , compared to the spin-lattice relaxation time, the  $90^\circ$  pulse nutates the reformed total magnetic moment vector of nearly maximum amplitude from the north pole down to the equatorial plane. Again a tail of nearly maximum value follows the  $90^\circ$  pulse. For intermediate values of  $\tau$  the tails will have smaller amplitudes. For one value in partic-



ular, which will be designated  $\tau_{\text{null}}$ , there will be no tail. Since the system relaxes or returns to equilibrium exponentially with the time constant  $T_1$ , it is easily shown that  $T_1$  may be calculated directly from the measured value of  $\tau_{\text{null}}$  by using the relation  $\tau_{\text{null}} = T_1 \ln 2$ . A  $180^\circ$  pulse at  $t = \tau + \tau_2$  will cause an echo to be formed at  $t = \tau + 2\tau_2$ . If  $2\tau_2 \ll T_2$  this echo may be used as an indicator of the growth of  $M_z$  from  $-M_0$  to  $M_0$ . The inhomogeneity of  $H_z$  plays no role in the decay and growth of the longitudinal component of the

polarization; diffusion and convection may here be ignored. One precaution must be noted, however. It has been assumed that each sequence of pulses is initiated only after the system has returned to thermal equilibrium. Thus if the above relation is used to compute  $T_1$ , the time interval between sequences must be large compared to  $T_1$ .

One of the authors (HYC) wishes to acknowledge many beneficial discussions with H. C. Torrey and P. R. Weiss during the latter period of this research.

### Beta-Ray Spectrum of $\text{Ag}^{110}$

TOSHIO AZUMA

*Physics Department, Naniwa University, Mozu, Sakai, Osaka, Japan*

(Received January 11, 1954)

The soft beta-ray spectrum of  $\text{Ag}^{110}$  has been measured by a double coil, magnetic lens beta-ray spectrometer, with a thin source and a thin counter window. From the analysis of the Fermi plot, three soft beta-ray groups of allowed type are found, with end points of 80 kev, 314 kev, and 530 kev. The ratio of their intensities is 10.7:3.2:15.3.

THE decay of  $\text{Ag}^{110}$  by the emission of three beta rays with end points of 87 kev, 530 kev, and 2.86 Mev, and of many groups of gamma rays, has been reported.<sup>1-8</sup> The difficulties involved in the analysis of these soft beta rays have also been pointed out.

In the present experiments the soft beta-ray spectrum has been measured by using a double coil, magnetic lens beta-ray spectrometer of about 2.0 percent resolving power. The detector consisted of a Geiger counter with a thin Zapon window which will detect electrons of energy 5 kev and higher. The source was prepared from radioactive solutions supplied from Oak Ridge. It has a surface density of not more than  $50 \mu\text{g}/\text{cm}^2$  on Zapon film of about  $30 \mu\text{g}/\text{cm}^2$ .

The spectrum consists of two low-energy groups of beta rays and many internal conversion lines of 116, 447, 618, 655, 687, 760, 759, 883, and 932 kev gamma rays, which were designated as strong and medium groups;<sup>1</sup> weak groups could not be detected because of the thin sample used in the present work. Since the Fermi plot of the spectrum of the 530-kev beta ray does not fit a straight line but is convex toward the

energy axis, we endeavored to fit various shape factors, as given by Konopinski and Uhlenbeck,<sup>9</sup> to these data. The ( $f$ ) value of this group is first forbidden. Then, in order to fit the data to a theoretically forbidden shape, it is necessary to multiply the allowed  $F(z,w)$  by a certain coefficient  $C_1$ , given by Konopinski and Uhlenbeck,<sup>9</sup> and see if the plot  $(N/C_1 \cdot F)^{\frac{1}{2}}$  against the total energy gives a straight line. The Fermi plots corrected with the correction factors of  $C_{1SV}/|\int \mathbf{r}|^2$  and  $C_{1TA}/|\Sigma B_{ij}|^2$  did not fit a straight line. We tried further to fit with various shape factors of second forbidden,  $C_{2SV}/|\Sigma R_{ij}|^2$ ,  $C_{2V}/|\Sigma A_{ij}|^2$ ,  $C_{2TA}/|\Sigma S_{ijk}|^2$ ,  $C_{2A}/|\Sigma T_{ij}|^2$ , and  $C_{2T}/|\Sigma A_{ij}|^2$ , where certain values of  $\Sigma S_{ijk}$  and  $\Sigma A_{ij}/\Sigma T_{ij}$  are assumed. But none of these corrected Fermi plots gave good results.

Therefore, we assume that the 530-kev beta-ray spectrum is complex, consisting of two groups. The best fit to the data for the Fermi plot is obtained in the energy range  $W \geq 1.60$  with  $W_0 = 2.038$ , where  $W$  is the energy in units of  $m_0c^2$  and  $W_0$  is the maximum energy in units of  $m_0c^2$ . The full shape of the 530-kev beta-ray group can be constructed from this straight line in the Fermi plot, which is shown in Fig. 1 as the  $\beta_3$  group. The differences between the measured and constructed values at each energy give the second beta-ray group which also fit a straight line in the Fermi plot in the energy range  $W \geq 1.23$ , with  $W_0 = 1.615$ . The full shape of this  $\beta_2$  group can also be constructed from the Fermi plot, as shown in Fig. 1. The remaining soft beta-ray group can also be con-

<sup>1</sup> Cork, Rutledge, Branyan, Stoddard, Childs, and LeBlanc, *Phys. Rev.* **80**, 286 (1950).

<sup>2</sup> K. Siegbahn, *Phys. Rev.* **75**, 1277 (1949); **77**, 233 (1950).

<sup>3</sup> F. Maienschein and J. L. Meem, *Phys. Rev.* **76**, 899 (1949).

<sup>4</sup> W. S. Emmerich and J. D. Kurbatov, *Phys. Rev.* **75**, 1446 (1949).

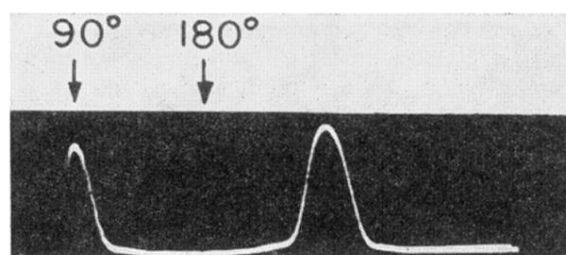
<sup>5</sup> W. Rall and R. G. Wilkinson, *Phys. Rev.* **71**, 321 (1947).

<sup>6</sup> W. C. Kelly, *Phys. Rev.* **85**, 101 (1952).

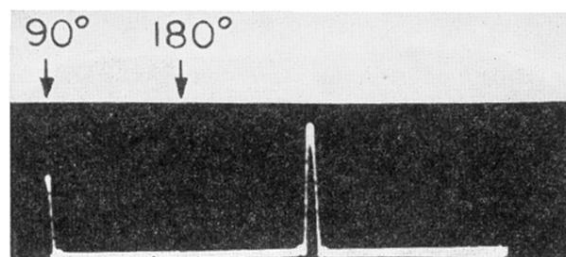
<sup>7</sup> Yu, Cheng, and Kurbatov, *Phys. Rev.* **75**, 1278 (1949).

<sup>8</sup> M. Goldhaber and R. D. Hill, *Revs. Modern Phys.* **24**, 179 (1952).

<sup>9</sup> E. J. Konopinski and G. F. Uhlenbeck, *Phys. Rev.* **60**, 308 (1941).



(A)



(B)

FIG. 4. Effect of the homogeneity of the field on the widths of tails and echoes. The tails and echoes associated with a sample (A) in a very homogeneous field are wide compared to those associated with a sample (B) in a less homogeneous field.

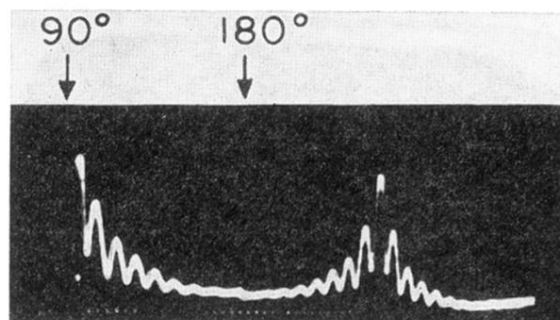
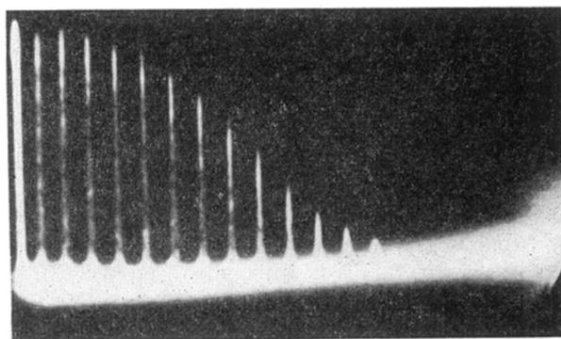
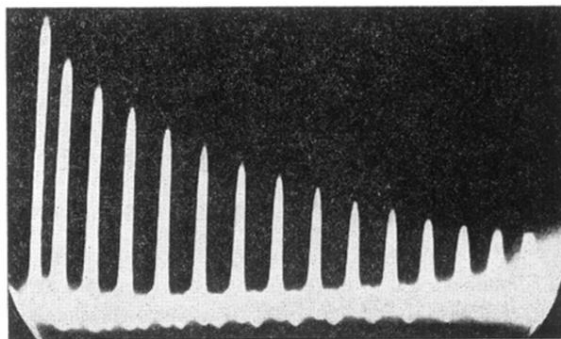


FIG. 5. A tail and echo associated with an acetic acid ( $\text{CH}_3\text{COOH}$ ) sample in a very homogeneous field. The nuclear signal displays modulation typical of the beating of two signals of nearly equal frequencies, the magnitude of one being three times that of the other. The beat frequency shown, corresponding to room temperature and 7000 gauss, is approximately 220 cps.



(A)



(B)

FIG. 7. (A) A "Method A" decay associated with water at 25°C. The time constant is approximately 0.2 sec. The decay is largely determined by the molecular diffusion through the 0.28 gauss/cm gradient. The decay is dominated by the factor  $\exp(-kt^2)$ . (B) A "Method B" decay associated with water at 25°C. The time constant of the decay is approximately 2.0 sec. The effect of diffusion has been largely circumvented.

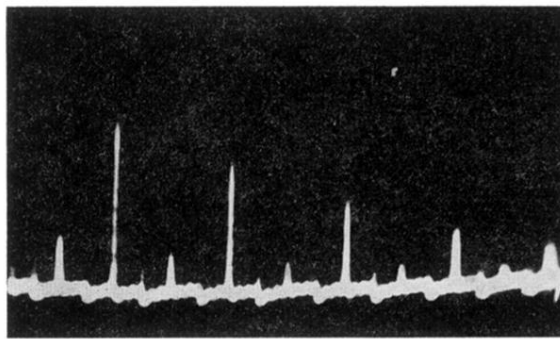


FIG. 8. The effect of molecular convection on a "Method *B*" decay. The odd-numbered echoes are much smaller than the even-numbered echoes.